# Sensitivity of water speeds to sea-bed roughness distribution in Minas Passage, Bay of Fundy

J. Culina[1] and R. Karsten

Department of Mathematics and Statistics
Acadia University
Wolfville, Nova Scotia, Canada
E-mail: [1] joel.culina@acadiau.ca

***Abstract***

**In the energetic tracts of coastal ocean suitable for tidal turbine deployment, the fast-flowing waters carve out a range of bedforms. In the Minas Passage of the Bay of Fundy, Canada, in which there are gigawatts of harnessable energy, the bathymetry obeys an approximate power-law relationship, such that, generally, the larger the bedform the more prominent it is. These roughness elements exert a significant (form) drag on the flow, such that their characteristic length scales impact the water speeds, and hence power potential, well up into the water column.**

**However, in numerical models of the coastal ocean used for resource assessment and turbine array optimisation, bottom roughness is crudely parameterised, usually as a spatial constant, and is adjusted (tuned) by trial-and-error with each change in model resolution. In this paper, we implement in a model of Minas Passage a resolution-independent, spatially-varying hydrodynamic roughness parameterisation, based on length scale information obtained from very high resolution bathymetry data, and discuss the implications for power potential and turbine placement.**

**Keywords:** hydrodynamic roughness, numerical modelling, power potential, tidal turbines.

## 1. *Introduction*

A default conception of the ocean floor is of a smoothly-varying, pebbled or sandy surface. This conception is codified in numerical models by treating the (unresolved component of the) sea-bed as an homogeneous momentum sink. In particular, a constant drag coefficient/roughness length scale is applied everywhere along the bottom boundary, under the assumption that heterogeneous sea-bed length scales directly affect only a shallow layer immediately above the sea-bed.

In the fast-flowing channels of interest for deployment of tidal turbines, this assumption is invalid. Rather, these energetic waters carve out bedforms that generate long wakes and significant form drag, the effects of which are felt through the entire water column. As it is a primary function of numerical models to provide detailed spatial coverage of power potential to complement sparse observations, it is crucial that these models capture the spatial heterogeneity arising from a varied and rough sea-bed. In this paper, we will discuss a method to systematically parameterise the hydrodynamic roughness length scale based solely on statistical properties of the sea-bed geometry.

## 2. *Observations in the Minas Passage*

The Minas Passage is a channel roughly 5 km wide, 15 km long and up to 170 m deep, connecting the Bay of Fundy to Minas Basin (**Figure 1**). Tidal ranges exceeding 15 m drive current speeds through Minas Passage exceeding 5 m/s. Large utility-scale tidal turbine farms are planned for the Passage, but to date only one turbine has been deployed. Studies [1] of realistic turbine placements in the Minas Passage have shown that there are gigawatts of energy that can be safely extracted.

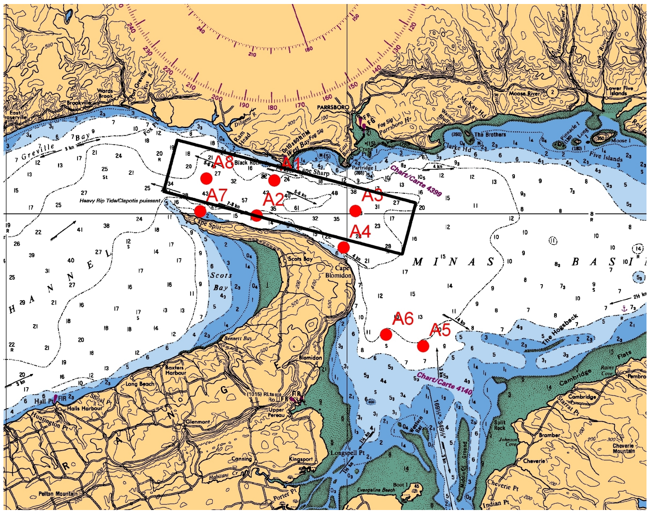


**Figure 1**: Minas Passage, Bay of Fundy, Nova Scotia, Canada. The red dots indicate the locations of ADCP deployments. The black box marks the approximate boundaries of the model domain used to derive the dimensionless roughness parameters (see Section 3).

Several Acoustic Doppler Current Profilers (ADCPs) have been deployed in Minas Passage, including at locations A1-A8 (**Figure 1)**. Using the measured current velocity profiles and the boundary layer equation:

$$u(z)=\frac{u_\tau}{\kappa}\log\left(\frac{z}{z_0}\right), \qquad (1)$$

where $u_\tau = C_D u_1$ is the friction velocity, the roughness parameters $C_D$ and $z_0$ may be deduced, and are shown in **Table 1** at locations A1, A3 and A8. These frictional parameters vary greatly among locations and are larger than 'standard' values such as $C_D = 5.0\times10^{-3}$ , indicating a strong, heterogeneous sink of momentum at the sea-bed.

| Mooring | A8 | A1 | A3 |
|---|---|---|---|
| $C_D(u_1)\cdot 10^{-3}$ | 42 | 21.6 | 6.2 |
| $z_0$(metres) | 0.13 | 0.06 | 0.006 |

**Table 1:** Bottom stress parameters inferred from ADCP measurements.

The reach of the bed stress is illustrated in **Figure 2**, depicting a non-dimensional profile of non-dimensional 'tidal current' speed at a potential tidal turbine site. At each vertical level, the tidal current series is the best fit to the ADCP-measured time series, using all statistically relevant tidal constituents (i.e., astronomical, shallow-water and long-term constituents). The near-collapse of points onto a single curve implies that horizontal speed approximately obeys the two-parameter boundary layer equation (1) through most of the water column. As this location is not atypical, much of the Minas Passage, *through much of the water column*, can be characterised as bottom boundary layer flow. Thus, based on observations, hydrodynamic bottom roughness is expected to influence the flow through much of the water column. Note that a tidal turbine will be subject to a large (but slowly-varying) vertical shear regardless of where it is placed in the water column.

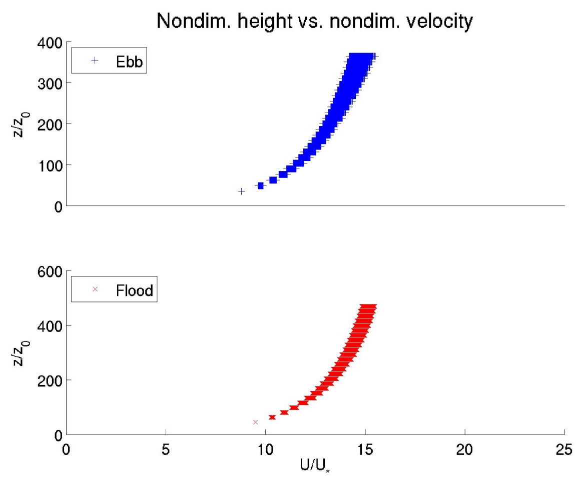


**Figure 2:** Non-dimensional profiles of non-dimensional speed for speeds greater than 2 m/s on ebb and flood tides at a potential tidal turbine site in Minas Passage.

The bottom roughness is evidently important but can it be readily characterised? As demonstrated in **Figure 3**, the bathymetry can indeed by broadly characterised as satisfying a height power-law spectra, $E_h(k)\sim k^\beta$, where $k$ is the radial wavenumber and $\beta<-1$. Thus, the bathymetry in Minas Passage has a similar appearance over a wide range of scales; i.e., it is 'self-similar'. Self-similarity has been widely documented in erosionally dissected landscapes [2], a classic example being a river and its families of tributaries. Evidently, the highly scoured sea-bed of Minas Passage organizes itself in a similar fashion. This compact power-law description of the sea-bed is exploited in the next section to a derive a simple formulation of spatially-varying hydrodynamic roughness.

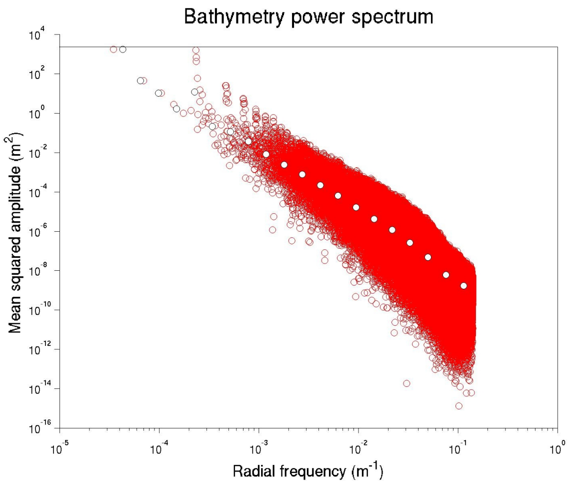


**Figure 3:** The 2-D power spectrum of bathymetry variations collapsed onto a 1-D plot. The white circles are the averages over bins of the raw spectrum.

## 3. *Spatially-varying hydrodynamic roughness*

### *3.1 Methodology*

In [3], a method is developed, for use in numerical models, for the parameterisation of *sub-grid scale* bottom roughness $z_0 = z_0(x, y)$ over realistic multi-scale surfaces, strictly in terms of statistics of the bottom geometry. The relationship between roughness elements and the overlying fluid has been studied extensively in an idealised setting of a uniform distribution of simply-shaped roughness elements (see [4] for a review), and for an arbitrary distribution of small roughness elements (e.g., paint, corrosion and fouling on a ship's hull [5]). In almost all cases, the focus has been on finding a single value of $z_0$ to quantify the effect of the entire surface. The theory in [3] applies to a surface with a power-law height spectra and represents the roughness as a spatially-varying field. As observations indicate (cf. Section 2), Minas Passage bathymetry has an approximate power-law spectra and an associated hydrodynamic roughness field with significant spatial variability.

The observed hydrodynamic roughness values in **Table 1** account for all length scales that contribute to the extraction of momentum at the ocean floor. In numerical modelling, equation (1) is commonly used as a slip condition to parameterise *unresolved* or *sub-grid* scale bottom stress. Hence, in this modelling context, $z_0$ is not generally the same as observed $z_0$; rather, modelled $z_0$ captures only the unresolved length scales contributing to bottom stress. If the model resolution is sufficiently coarse, then observed and modelled $z_0$ are the same. However, method [3] assumes that the model resolves some of the bottom drag, through, e.g., form drag caused by flow separation off of resolved bathymetry, with the remainder of the drag parameterised through $z_0$. Generally, the greater the model resolution (i.e., the more bathymetry and fluid flow is resolved), the greater the resolved form drag, such that (model) $z_0$ is generally resolution dependent. Nevertheless, this method assumes that $z_0$ is derived strictly in terms of unresolved bottom geometry and a dimensionless parameter $\alpha$ according to:

$$z_0 = \alpha \sigma_h , \sigma_h(x, y) = \left( \overline{(h - \tilde{h})^2} \right)^{1/2} . \quad (2)$$

Here, *h* is the bathymetry and $\widetilde{()}$ is a low-pass filter. The parameter $\alpha$ is determined for a given surface *independent of model resolution*, in the fashion illustrated below. Hence, each time the resolution is changed (e.g., by changing the filter cut-off frequency), it is only necessary to calculate the root-mean-square of high-pass filtered bathymetry in order to determine the new spatially-varying roughness field. This formula is a simplification of the empirically derived formula in [5], which relates bottom drag to additional, higher moments of surface geometry, particularly surface skewness.

The parameter $\alpha$ is found by enforcing the condition that the total (resolved and unresolved) bottom drag force does not change with a change in model resolution. As mentioned, it is generally the case that the greater the model resolution, the greater the resolved drag. Following from the equation for the standard deviation of sub-grid scale bathymetry, $\sigma_h$, the greater the model resolution, the less the unresolved drag. The condition of resolution independence is then enforced by using the value of $\alpha$ for which the total drag at one resolution equals that at another resolution. Since self-similarity of length scales is implied by the power-law spectra of the bathymetry, this value of $\alpha$ should not depend on the two resolutions compared. In [3], using idealised height power-law spectra in a large-eddy simulation of the atmospheric boundary layer, a resolution-independent value of $\alpha$ was found, which was applied in boundary condition (1) to derive resolution-independent velocity fields.

### *3.2 Implementation in Minas Passage model*

Although [3] uses a constructed topography with a height power-law spectrum, Minas Passage bathymetry broadly satisfies such a spectrum. However, there are a number of considerations in adapting this method to Minas Passage, and to real-world flows in general. In particular, determining $\alpha$ in practice requires that a sufficiently simple model balance is achieved, as in [3] between the pressure gradient and bottom drag forces. This is not to say that such a balance is required in nature, as it is certainly the case that acceleration plays a pivotal role in the Minas Passage dynamical balance. Rather, it is assumed that the dimensionless parameter $\alpha$ derived under simpler conditions is the same as it would be derived under fully realistic conditions. A necessary simplification is the elimination of shorelines and headlands, particularly, the elimination of the associated form drag. Headland-generated eddies have been observed to have a dominant retarding influence on channel flow [6], which becomes better realised in numerical models as model, and hence eddy, resolution is increased. Using the constraint that total drag is resolution independent with one free parameter scaling the unresolved bathymetry deviations, $\alpha$ would account for changes in form drag arising from both the sea bed and headlands. Hence, such a constraint can only be applied with headlands and shorelines removed, such that the primary source of drag in the channel is ocean floor drag.

A model grid of Minas Passage without shorelines, and generally without any side-wall flow separation, was created with a rectangular domain that covers most of Minas Passage without crossing shoreline (black box in **Figure 1**, and **Figure 4**). Simulations were conducted using the Finite Volume Community Ocean Model (FVCOM) [7]. High-resolution (5 metre) bathymetry collected by the Geological Survey of Canada was used throughout the Minas Passage. As the eastern (Minas Basin) and western (Minas Channel) ends of the model domain are approached, true, shallow water depths are replaced by deepening values, so that instead of the necessary water volume funnelling in from and out to wider bodies of water (as in reality), water is funnelled in from and out to deeper waters. The rectangular shape prevents flow separation along side walls, and also allows for easier manipulation, particularly by allowing filtering with a 2-D FFT. The artificial bathymetry at the ends is connected smoothly with the true bathymetry and bathymetry variations are tapered to prevent large wakes from forming

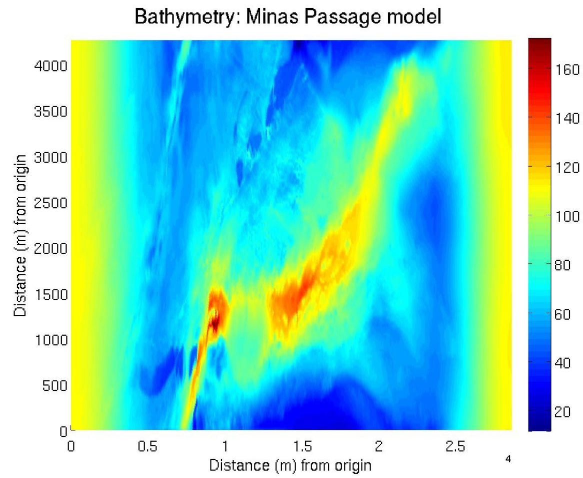


**Figure 4:** Bathymetry of the Minas Passage model, with model domain approximately corresponding to the region outlined by the black box in **figure 1**. Along-channel/x-axis scaling is approximately 1/8 the cross-channel/y-axis scaling.

towards the ends (and potentially dominating the force balance).

The bathymetry in the Minas Passage model is resolved with terrain-following σ-coordinates, whereas the 'resolved' bathymetry in [3] is, in fact, parameterised. Obviously, the representation of the resolved bathymetry is much more realistic in the Minas Passage model. Wakes are visible behind roughness elements at sufficiently high resolution (not shown), indicating the presence of resolved drag.

**Figure 5** demonstrates the impact on water speeds of spatially-varying bottom roughness by depicting the difference between depth-averaged fluid speeds over heterogeneous and homogeneous roughness. Spatially-varying roughness is found using equation (2) for $\sigma_h$, but with a scaling parameter that yields steady-state speeds of 2.5-3.5 m/s, rather than systematically finding $\alpha$ according to the condition of resolution-independent total drag (the reason for this choice of $\alpha$ is discussed below). The homogeneous hydrodynamic roughness length scale is set to be the spatial average of the heterogeneous roughness. Each structured grid has a resolution of 30 metres, and steady leftward (westward, ebb) flow is obtained by introducing a constant tidal head of 0.5 metres at the right (eastern) boundary.

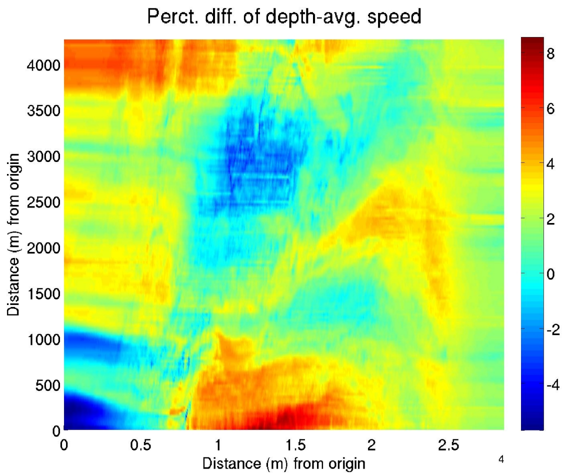


**Figure 4:** Percent differences of depth-averaged speed between numerical simulations with constant hydrodynamic roughness and with spatially-varying roughness.

The grouping of colours within the difference plot suggests that there is a significant component of the difference field that changes slowly in space. This would cause significant phase differences between tidal constituents derived over the different surfaces; for example, near the lateral boundaries of the mid-plot, bluish-coloured region, flow over constant roughness would be significantly lagging flow over the spatially-varying roughness. The finer scale differences are obviously crucial in turbine micro-siting studies. Within the first 10 metres above the sea-bed, where (parts of) turbines will be located, maximum speed differences are between 15-20% (not shown).

## 4. Discussion and Summary

The effect of sea-bed drag on turbine power potential is greatly underappreciated in modelling studies, which effectively treat the sea-bed as a slightly roughened, uniform surface. However, observations in Minas Passage, Bay of Fundy, where there is planned a utility-scale turbine deployment, show that hydrodynamic roughness has significant spatial variability, with an impact on flow speeds that extends through the entire water column. A resolution-independent parameterisation for spatially-varying roughness based solely on the standard deviation of the bathymetry was adapted for use in open channel flows. Using an appropriately designed model of Minas Passage, the effect of properly modelled roughness on power potential through the water column was quantified.

Continuing with this work, an idealised model with (perfect) power-law bathymetry has been constructed to improve adaption of the method [3], which was designed for atmospheric flows, to an open channel with a free surface. Subsequently, a value of $\alpha$ will be derived from the Minas Passage model and applied to a full Bay of Fundy model, and comparison will be made with a wide suite of observations. Subsequent work will focus on the effect of roughness elements on the dissipation of turbine wakes, and hence on turbine placement.

## Acknowledgements

We would like to thank the Offshore Energy Research Association of Nova Scotia for financial support, the Atlantic Computational Excellence Network for computational and financial support, and John Shaw, Geological Survey of Canada, for providing bathymetry data.

## References

[1] R. Karsten, A. Swan, and J. Culina. (2012): Assessment of arrays of in-stream tidal turbines in the Bay of Fundy. *Phil. Trans. Roy. Soc. A*, in press.

[2] J. Perron, J. Kirchner and W. Dietrich. (2008): Spectral signatures of characteristic spatial scales and nonfractal structure in landscapes. *J. Geophys. Res.*, **113**, F04003.

[3] W. Anderson and C. Meneveau. (2011): Dynamic roughness model for large-eddy simulation of turbulent flow over multiscale, fractal-like rough surfaces. *J. Fluid Mech.*, **679**, 288-314.

[4] J. Jiménez. (2004): Turbulent flow over rough walls. *Ann. Review Fluid Mech.*, **36**, 173-196.

[5] K. Flack and M. Schultz. (2010): Review of hydraulic roughness scales in the fully rough regime. *ASME J. Fluids Eng.*, **132**, 041203 (1-10).

[6] R. McCabe and P. MacCready. (2006): Form drag due to flow separation at a headland. *J. Phys. Ocean.*, **36**, 2136-2152.

[7] C. Chen, H. Huang, R. Beardsley, H. Liu, Q. Xu and G. Cowles. (2007): A finite-volume numerical approach for coastal ocean circulation studies: comparisons with finite difference models. *J. Geophys. Res.*, **112**, C03018.